

# Cyclin-Dependent Kinase Inhibitor 2A is a Key Regulator of Cell Cycle Arrest and Senescence in Endothelial Colony-Forming Cells in Moyamoya Disease

Seung Ah Choi,<sup>1,2</sup> Youn Joo Moon,<sup>1,2</sup> Eun Jung Koh,<sup>1,2</sup> Ji Hoon Phi,<sup>1,2,3</sup> Ji Yeoun Lee,<sup>1,2,4</sup> Kyung Hyun Kim,<sup>1,2</sup> Seung-Ki Kim<sup>1,2,3</sup>

*Division of Pediatric Neurosurgery,<sup>1</sup> Pediatric Clinical Neuroscience Center, Seoul National University Children's Hospital, Seoul, Korea  
Department of Neurosurgery,<sup>2</sup> Seoul National University Hospital, Seoul National University College of Medicine, Seoul, Korea  
Neuroscience Research Institute,<sup>3</sup> Seoul National University College of Medicine, Seoul, Korea  
Department of Anatomy,<sup>4</sup> Seoul National University College of Medicine, Seoul, Korea*

**Objective :** Endothelial colony-forming cells (ECFCs) have been reported to play an important role in the pathogenesis of moyamoya disease (MMD). We have previously observed stagnant growth in MMD ECFCs with functional impairment of tubule formation. We aimed to verify the key regulators and related signaling pathways involved in the functional defects of MMD ECFCs.

**Methods :** ECFCs were cultured from peripheral blood mononuclear cells of healthy volunteers (normal) and MMD patients. Low-density lipoproteins uptake, flow cytometry, high content screening, senescence-associated  $\beta$ -galactosidase, immunofluorescence, cell cycle, tubule formation, microarray, real-time quantitative polymerase chain reaction, small interfering RNA transfection, and western blot analyses were performed.

**Results :** The acquisition of cells that can be cultured for a long time with the characteristics of late ECFCs was significantly lower in the MMD patients than the normal. Importantly, the MMD ECFCs showed decreased cellular proliferation with G1 cell cycle arrest and cellular senescence compared to the normal ECFCs. A pathway enrichment analysis demonstrated that the cell cycle pathway was the major enriched pathway, which is consistent with the results of the functional analysis of ECFCs. Among the genes associated with the cell cycle, cyclin-dependent kinase inhibitor 2A (CDKN2A) showed the highest expression in MMD ECFCs. Knockdown of CDKN2A in MMD ECFCs enhanced proliferation by reducing G1 cell cycle arrest and inhibiting senescence through the regulation of CDK4 and phospho retinoblastoma protein.

**Conclusion :** Our study suggests that CDKN2A plays an important role in the growth retardation of MMD ECFCs by inducing cell cycle arrest and senescence.

**Key Words :** Moyamoya disease · Endothelial colony-forming cells · Cyclin dependent kinase inhibitor 2A · Cell cycle · Cellular senescence.

• Received : January 6, 2023 • Revised : March 17, 2023 • Accepted : April 22, 2023

• Address for correspondence : **Seung-Ki Kim**

Division of Pediatric Neurosurgery, Seoul National University Children's Hospital, 101 Daehak-ro, Jongno-gu, Seoul 03080, Korea  
Tel : +82-2-2072-3084, Fax : +82-2-744-8459, E-mail : [nstomas@snu.ac.kr](mailto:nstomas@snu.ac.kr), ORCID : <https://orcid.org/0000-0002-0039-0083>

This is an Open Access article distributed under the terms of the Creative Commons Attribution Non-Commercial License (<http://creativecommons.org/licenses/by-nc/4.0>) which permits unrestricted non-commercial use, distribution, and reproduction in any medium, provided the original work is properly cited.

## INTRODUCTION

Moyamoya disease (MMD) is a cerebrovascular disorder characterized by progressive occlusion of the major cerebral arteries and compensatory arterial collateral vessels at the base of the brain<sup>1,10</sup>. MMD occurs worldwide, and its prevalence is highest in East Asia, including Korea, Japan, and China<sup>21</sup>. Genetic abnormalities or physical damage to major cerebral arteries are suggested to be the pathogenesis of MMD<sup>1,4</sup>. Ring finger protein 213 (RNF213) has been reported as a susceptibility gene of MMD<sup>13,21</sup>, but its biological function has not yet been fully elucidated.

Endothelial progenitor cells (EPCs) play a major role in vascular homeostasis, neovascularization, and re-endothelialization<sup>24</sup>. EPCs are generally divided into two distinct types according to the phenotypic lineage, namely, the hematopoietic lineage (early EPCs or myeloid angiogenic cells) and endothelial lineage (late EPCs or endothelial colony-forming cells [ECFCs])<sup>2,15</sup>. ECFCs were found to be involved in the physiological process of neovascularization and subsequent pathological events, such as hypertension, myocardial infarction, stroke, and atherosclerosis<sup>28</sup>.

Many studies have shown that ECFCs play an important role in the pathogenesis of MMD. Previous studies suggested that the proliferation ability of MMD ECFCs in childhood was decreased, thus showing impaired functional activity<sup>2,9</sup>. We previously reported that MMD ECFCs have reduced tube formation and an increased senescence-like phenotype<sup>9</sup>. In addition, we performed a microarray analysis and found that biological processes related to the cell cycle and DNA repair were inhibited in MMD ECFCs compared to normal ECFCs<sup>12</sup>. In this study, we hypothesized that MMD ECFC dysfunction could be the result of accelerated senescence and cell cycle arrest and performed experiments to reveal the key genes in this process.

## MATERIALS AND METHODS

### Study subjects

The diagnosis of MMD was made by brain magnetic resonance angiography or cerebral angiography. Healthy volunteers who had no history of stroke, hypertension, or smoking were recruited. Blood from MMD patients and normal con-

trols were obtained with informed consent under Institutional Review Board (IRB) approval (IRB No. 1706-142-862). As this study used cells from a cell bank, patient consent was waived from the Ethics Review Committee.

### ECFC cultures

Peripheral blood mononuclear cells (PBMNCs) were isolated from the venous peripheral blood of MMD (n=468) and normal (n=64) by density gradient centrifugation. PBMNCs were seeded on a collagen-coated plate (BD Biosciences, San Jose, CA, USA) with endothelial cell growth media (EGM-2; Clonetics, San Diego, CA, USA) as described in previous paper<sup>3,9,18</sup>. Cells displaying cobblestone morphology were expanded and subcultured in collagen-coated dishes. All cells were maintained at 37°C in a humidified atmosphere containing 5% CO<sub>2</sub> and used at passage 6. For the *in vitro* functional analysis, we conducted further experiments using cells that exhibited the cobblestone morphology, low-density lipoprotein (LDL) uptake, and surface marker expression, which correspond to the characteristics of ECFCs (3 or more cases per group, Supplementary Table 1).

### Colony-forming unit assays

PBMNCs ( $1 \times 10^7$ ) were plated on a 6-well collagen-coated plate. After 7–14 days, the number of clusters was manually counted using light microscopy by counting five random microscopic fields<sup>3,9,18</sup>.

### Dil-ac-LDL uptake

The cells ( $5 \times 10^4$ ) plated on an 8-well chamber glass microscope slide (Lab Tek II; Thermo Fisher, Waltham, MA, USA) and incubated in media containing 10 µg/mL Dil-ac-LDL for 4 hours. The cells were then washed and fixed with 2% paraformaldehyde at room temperature. The cells were observed using a fluorescence microscope as described previously<sup>9,12,18</sup>.

### Flow cytometric analysis

ECFCs ( $1 \times 10^6$ ) were characterized by flow cytometry, and antibodies against human CD31 kinase insert domain receptor (KDR), CD14, and CD45 (Miltenyi Biotec, Bergisch Gladbach, Germany) were used. Mononuclear cells were selected using a gate to exclude residual granulocytes, cell debris, and small particles, and 10000–50000 cells were acquired per sample<sup>9,18</sup>. Flow cytometric analysis was performed using

FACScas flow cytometry (Becton Dickinson, Franklin Lakes, NJ, USA), and the data were analyzed with FlowJo software (FlowJo LLC, Ashland, OR, USA).

### High content screening (HCS) analysis

A real-time live-cell analysis of the ECFCs was performed using HCS. The cells ( $2 \times 10^4$ ) were seeded in 96-well plates (Cell-Carrier-96 Ultra; PerkinElmer, Waltham, MA, USA) and incubated in a HCS system (Operetta CLS; PerkinElmer). Live and dead cells were labeled using the HCS LIVE/DEAD Green Kit (Thermo Fisher Scientific, Eugene, OR, USA) according to the manufacturer's instructions. The cell proliferation rate with doubling time was determined by the HCS system<sup>16,27</sup>.

### Senescence-associated $\beta$ -galactosidase assay

ECFCs ( $1 \times 10^5$ ) were incubated in 6-well plates, washed in phosphate-buffered saline (PBS), and then fixed for 10–15 minutes at room temperature with 0.5 mL of a fixative solution. After washing, the cells were incubated overnight with the staining solution at 37°C<sup>17</sup>. SA- $\beta$ -gal assays were performed using a cellular senescence assay kit (Merck, Billerica, MA, USA) according to the manufacturer's instructions. The cells were observed under a microscope at a magnification of  $\times 40$ . The number of  $\beta$ -galactosidase-positive cells (blue) within three randomly selected hotspots was quantified. Quantitative analysis was performed by two observers blinded to all groups through data collection.

### Immunofluorescence assay

The cells ( $5 \times 10^4$ ) were seeded onto an 8-well chamber glass and immunofluorescence assays were carried out as described previously<sup>3,17,18</sup> using anti-Caspase-3 (Merck, Darmstadt, Germany; 1 : 100) antibody. The cells were mounted with VECTASHIELD<sup>®</sup> Antifade Mounting Medium with 4',6'-diamidino-2-phenyl-indole (DAPI; Vector Laboratories, Newark, CA, USA) and observed using a fluorescence microscope. The number of Caspase-3-positive cells (green) counterstained with DAPI (blue) within in three randomly chosen hotspots was quantified by two independent observers.

### Cell cycle analysis

ECFCs ( $2 \times 10^5$ ) were fixed with ice-cold 70% ethanol before incubation with PI solution (50  $\mu$ g/mL PI, 0.2 mg/mL RNase A) at 37°C for 40 minutes and then resuspended in 500  $\mu$ L of

PBS for flow cytometry analysis using a FACScan flow cytometer (BD Biosciences)<sup>9,12,18</sup>.

### Tube formation assay

The cells ( $2 \times 10^4$ ) were incubated in Matrigel-coated 48-well plates (BD Biosciences) and then incubated as described previously<sup>6,9,18</sup>. The number of tubes and branches were counted using a fluorescence microscope counted at three random microscopic fields by two independent observers.

### Functional enrichment analysis

Data from a microarray gene expression analysis conducted in our previous study<sup>12</sup> were used to further determine the biological functions. Significant differentially expressed genes were selected with threshold criteria of  $|\log FC| \geq 1$  and  $p < 0.05$  by comparing normal and MMD ECFCs and used for the functional enrichment analysis. Biological process analysis was performed using Functional Enrichment analysis tool (FunRich) software (version 3.1.3; www.funrich.org)<sup>14,22</sup>.

### Real-time quantitative polymerase chain reaction (RT-qPCR)

Total RNA was isolated using miRNeasy mini kits (Qiagen GmbH, Hilden, Germany). The integrity and concentration of RNA were confirmed by an Agilent Bioanalyzer (Agilent Technologies, Santa Clara, CA, USA) and NanoDrop spectrophotometer (NanoDrop Technologies, Wilmington, DE, USA), respectively. mRNA expression was validated by RT-qPCR using SYBR green in an ABI7500 system (Applied Biosystems, Carlsbad, CA, USA) as described previously<sup>12</sup>. The primer sequences are described in Supplementary Table 2. The comparative threshold cycle ( $\Delta Ct$ ) method was used to calculate the relative gene expression normalized to glyceraldehyde 3-phosphate dehydrogenase.

### Small interfering RNA (siRNA) transfection

siRNAs were used for the knockdown of CDKN2A gene expression in MMD ECFCs ( $n=3$  per group). Negative control (NC)-siRNA and CDKN2A-siRNA (sense : 5'-UGUCCUGCCUUUUUAAACGUAtt, antisense : 5'-UACGUUAAAAGGCAGGACAtt) were purchased from Ambion (Carlsbad, CA, USA). Transfection was performed using Lipofectamine RNAiMAX (Invitrogen, Carlsbad, CA, USA) as described previously<sup>18</sup>. The knockdown efficiency of CDKN2A-siRNA was confirmed by

RT-qPCR and western blot analysis.

### Cell viability assay

The cells ( $1 \times 10^4$ ) were seeded in 96-well plates after siRNA transfection and cell viability was performed using EZ-cytox (Daeil Lab, Seoul, Korea) as described previously<sup>6)</sup>. The results are revealed as a percentage of cell viability for the CDKN2A-siRNA-treated cells compared with the NC-siRNA-treated cells.

### Western blot

Total proteins were extracted with RIPA buffer (GenDEPOT, Barker, TX, USA). Western blot analysis was performed as described previously<sup>18)</sup>. The primary antibodies used were as follows: anti-CDKN2A (Santa Cruz Biotechnology, Dallas, TX, USA; 1 : 1000), anti-CDKN1A (Cell Signaling Technology [CST], Beverly, MA, USA; 1 : 500), anti-CDK2 (CST; 1 : 1000), anti-CDK4 (CST; 1 : 1000), anti-CDK6 (CST; 1 : 1000), pRBI (CST; 1 : 1000), and anti- $\beta$ -actin (Sigma-Aldrich, Saint Louis, MO, USA; 1 : 5000). Western blot densitometry and relative intensity of protein bands calculated using image J software (version 1.53k; National Institutes of Health, Bethesda, MD, USA). Densitometric analysis of band intensities was performed, normalized to internal  $\beta$ -actin expression level and values were calculated relative to NC-siRNA.

### Statistical analysis

All values were calculated as the mean  $\pm$  standard deviation (SD) or expressed as a percentage  $\pm$  SD of the controls from at least three independent experiments. Student's t test and the Mann-Whitney test were used to compare continuous variables between two groups. *p*-values  $< 0.05$  were considered statistically significant. All statistical analyses were performed using GraphPad Prism software (La Jolla, CA, USA).

## RESULTS

### Characterization of ECFCs

The total number of PBMNCs isolated from normal or MMD patients did not significantly differ ( $p > 0.05$ ). However, a much lower rate of differentiation into ECFCs was observed for MMD PBMNCs compared with normal PBMNCs (Table 1). Interestingly, when cells obtained from normal and MMD PBMNCs formed colonies (Supplementary Fig. 1A), they displayed a cobblestone morphology (Supplementary Fig. 1B) and ac-LDL uptake (Supplementary Fig. 1C), which are characteristics of ECFCs. These cells positively expressed ECFCs markers, including CD31 (99.67%  $\pm$  0.41% in normal ECFCs, 98.34%  $\pm$  3.17% in MMD) and KDR (78.39%  $\pm$  12.98% in normal ECFCs, 67.03%  $\pm$  26.32% in MMD ECFCs). On the other hand, the expression of the monocyte marker CD14 (2.20%  $\pm$  1.43% in normal ECFCs, 1.66%  $\pm$  1.30% in MMD ECFCs) and the hematopoietic marker CD45 (2.28%  $\pm$  0.57% in normal ECFCs, 1.26%  $\pm$  0.60% in MMD ECFCs) was very low (Supplementary Table 3).

### Defective functions of MMD ECFCs

We performed *in vitro* real-time imaging by HCS to estimate cell proliferation and doubling time. Normal ECFCs showed increased cell numbers over time, whereas the MMD ECFCs exhibited stagnant cell proliferation (Fig. 1A). The doubling time in MMD ECFCs was 7.2-fold longer than that of normal ECFCs (normal vs. MMD : 63.1  $\pm$  33.9 hours vs. 454.8  $\pm$  559.6 hours,  $p < 0.05$ ; Fig. 1B). Importantly, decreased proliferation of MMD ECFCs was observed with G1 arrest (normal vs. MMD : 63.3%  $\pm$  6.6% vs. 86.0%  $\pm$  3.4%,  $p < 0.01$ ; Fig. 1C) and cellular senescence (normal vs. MMD : 1.8  $\pm$  0.5 vs. 63.4  $\pm$  11.9,  $p < 0.001$ ; Fig. 1D and E). There was no difference in

**Table 1.** Information of the differentiation and expansion of endothelial colony-forming cells (ECFCs) from peripheral blood mononuclear cells (PBMNCs)

Group	Gender	Average age (years)	RNA213 variant	PBMNC counting	Rate of differentiation into ECFCs	Maintained after differentiation (>6 passages)
Normal controls	F, 29; M, 35	23.8 $\pm$ 1.0 (range, 20 to 30 years)	GG, 64; GA, 0; AA, 0	$2.3 \times 10^7 \pm 5.4 \times 10^6$	95.31%; 61 out of 64 cases	32.79%; 20 out of 61 cases
MMD patients	F, 251; M, 217	8.4 $\pm$ 0.8 (range, 7 months to 19 years)	GG, 58; GA, 154; AA, 10; unidentified, 264	$2.1 \times 10^7 \pm 1.1 \times 10^7$	19.66%; 92 out of 468 cases	13.04%; 12 out of 92 cases

F : female, M : male, GG : wild types, GA : heterozygotes, AA : homozygotes, MMD : Moyamoya disease

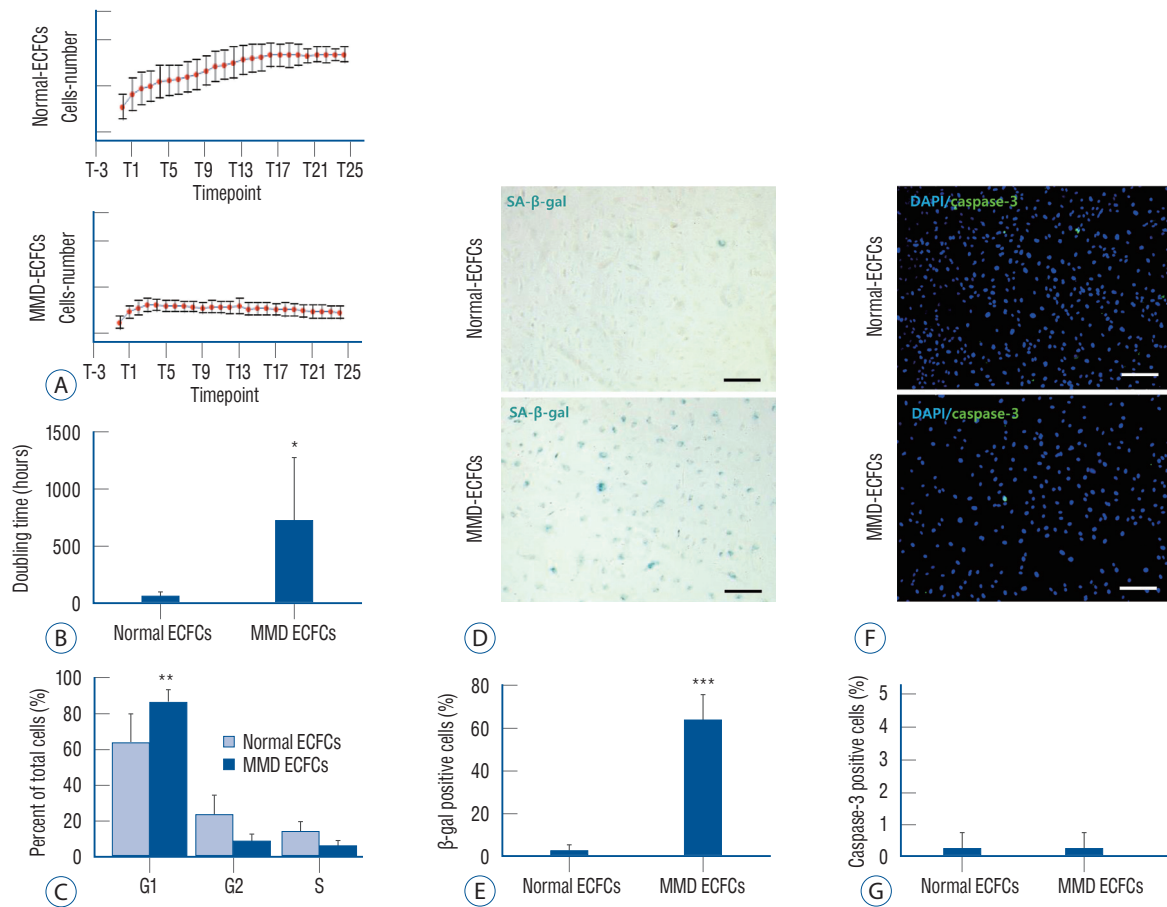


**Fig. 1.** Cell growth arrest and senescence of MMD ECFCs. A : Cell proliferation is assessed via a high-throughput screening (HCS) assay. Representative growth curves (nonexpanded cells) of ECFCs are generated from cell images taken every 4 hours using the imaging system and its cell density algorithm. B : Doubling time results suggest that MMD ECFCs are significantly slower than normal ECFCs. C : Cell cycle analysis by flow cytometry shows that G1 arrest is higher in MMD ECFCs than in normal ECFCs. D and E : Senescence-associated  $\beta$ -galactosidase (SA- $\beta$ -gal) staining ( $\times 100$ ) reveals more SA- $\beta$ -gal-positive cells in MMD ECFCs than in normal ECFCs. F and G : In both MMD ECFCs and normal ECFCs, few caspase-3-positive cells are observed ( $\times 100$ ). Scale bars : 100  $\mu$ m. \* $p < 0.05$ , \*\* $p < 0.01$ , and \*\*\* $p < 0.001$ . ECFCs : endothelial colony-forming cells, MMD : Moyamoya disease. DAPI : 4',6-diamidino-2-phenylindole.

apoptosis (normal ECFCs vs. MMD ECFCs :  $0.2\% \pm 0.5\%$  vs.  $0.3\% \pm 0.5\%$ ,  $p > 0.05$ ; Fig. 1F and G). Moreover, the MMD ECFCs lacked the ability to form normal capillary-like structures on Matrigel (normal vs. MMD :  $16.3 \pm 3.4$  vs.  $3.7\% \pm 1.7\%$ ,  $p < 0.001$ ; Supplementary Fig. 1D and E). These results suggest that ECFCs isolated from MMD patients have functional defects.

### Biological pathway of cell cycle-associated CDKN2A in MMD ECFCs

We reanalyzed biological pathways using previously obtained microarray data<sup>12</sup> based on FunRich software. We found that the top five major biological pathways in the MMD

ECFCs included the cell cycle, DNA replication, mitotic M-M/G1 phases, interferon signaling and interferon-alpha/beta signaling. The cell cycle pathways were mostly enriched pathways in MMD ECFCs compared with normal ECFCs (20.7%,  $p < 0.001$ ; Fig. 2A). We verified the expression of cell cycle-related genes through RT-qPCR. Among these genes, only CDKN2A was significantly increased in the MMD ECFCs ( $p < 0.05$ , Fig. 2B).

### Role of CDKN2A in MMD ECFCs

To determine whether the cell cycle and senescence are regulated by CDKN2A in MMD ECFCs, we used CDKN2A-siRNA. Transfection of CDKN2A-siRNA effectively reduced



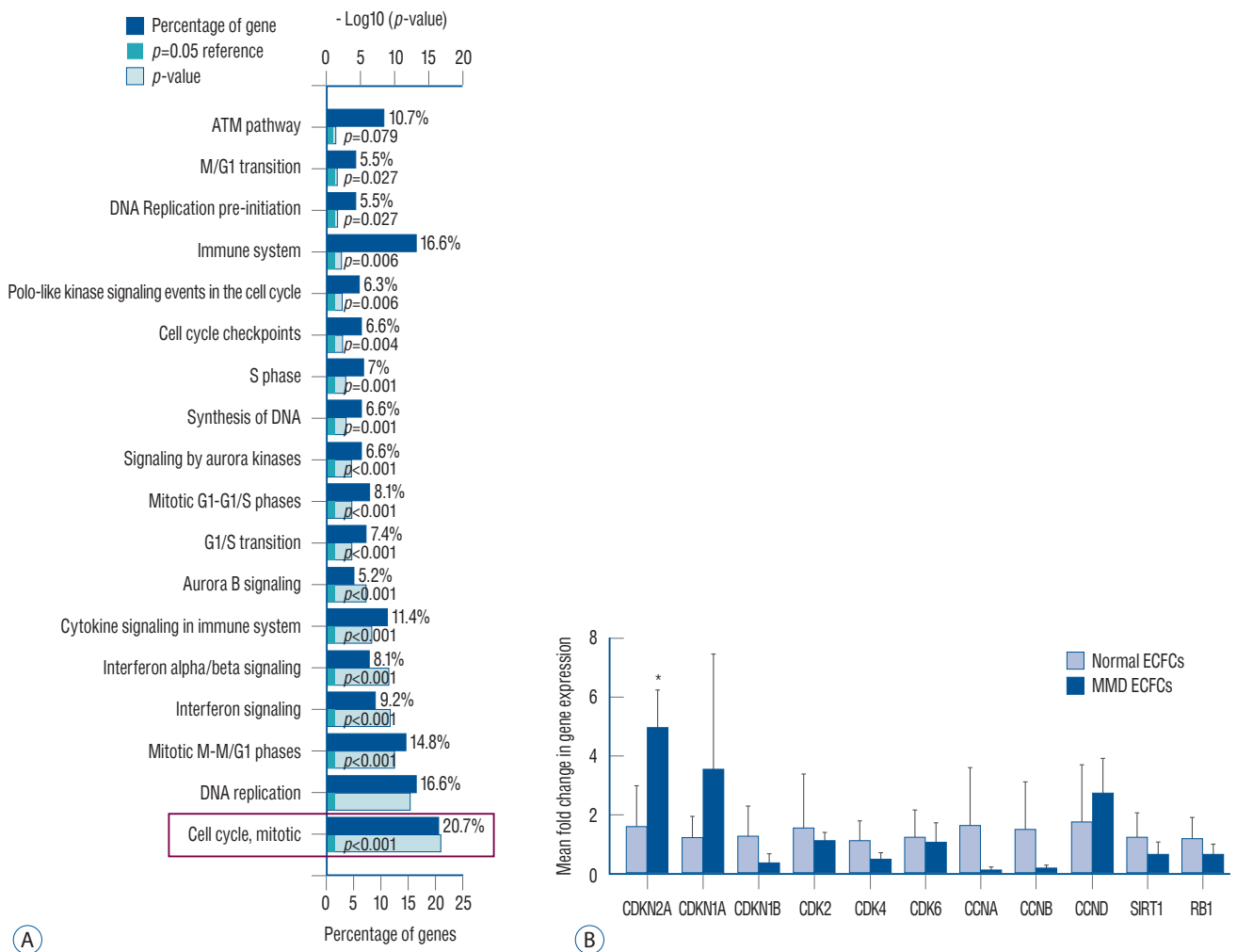


**Fig. 2.** Analysis of the major biological pathways of MMD ECFCs and verification of the associated genes. A : Functional gene enrichment analysis of identified differentially expressed genes (DEGs) as biological pathways. B : Validation of cell cycle-related genes by RT-qPCR. \* $p<0.05$ . ATM : ataxia telangiectasia mutated, ECFCs : endothelial colony-forming cells, MMD : Moyamoya disease, CDKN : cyclin-dependent kinase inhibitor, CCNA : cyclin A, CCNB : cyclin B, CCND : cyclin D, SIRT1 : sirtuin 1, RB1 : retinoblastoma, RT-qPCR : real-time quantitative polymerase chain reaction.

CDKN2A mRNA expression by 70% at 48 hours (NC-siRNA vs. CDKN2A-siRNA :  $1.0\pm 0.1$  vs.  $0.3\pm 0.3$ ,  $p<0.001$ ; Fig. 3A). The knockdown of CDKN2A significantly improved the viability of the MMD ECFCs (NC-siRNA vs. CDKN2A-siRNA :  $100.0\%\pm 7.9\%$  vs.  $141.5\%\pm 20.4\%$ ,  $p<0.001$ ; Fig. 3B). The knockdown of CDKN2A in the MMD ECFCs prevented G1 arrest (NC-siRNA vs. CDKN2A-siRNA :  $85.9\%\pm 4.0\%$  vs.  $76.5\%\pm 3.8\%$ ,  $p<0.001$ ; Fig. 3C and D) and cellular senescence (NC-siRNA vs. CDKN2A-siRNA :  $63.4\%\pm 11.9\%$  vs.  $0.5\%\pm 0.6\%$ ,  $p<0.001$ ; Fig. 3E and F), but did not significantly affect apoptosis (NC-siRNA vs. CDKN2A-siRNA :  $0.3\%\pm 0.4\%$  vs.  $1.0\%\pm 1.1\%$ ,  $p>0.05$ ; Fig. 3G and H). Importantly, the knockdown of CDKN2A improved the tubule formation ability of

the MMD ECFCs by 1.7-fold ( $p<0.001$ , Fig. 3I). Collectively, these results suggest that inhibition of CDKN2A in MMD ECFCs enhances the cell growth and tubule formation ability of MMD ECFCs through regulation of G1 arrest and cellular senescence.

### Signaling pathways regulated by CDKN2A

We investigated the cell cycle and senescence-related signaling pathways by CDKN2A inhibition in MMD ECFCs. We confirmed that CDKN2A protein expression was effectively reduced by CDKN2A-siRNA in the MMD ECFCs (NC-siRNA vs. CDKN2A-siRNA :  $1.00\pm 0.08$  vs.  $0.51\pm 0.21$ ,  $p<0.05$ ; Fig. 4A). Next, we checked whether CDKN2A was negatively

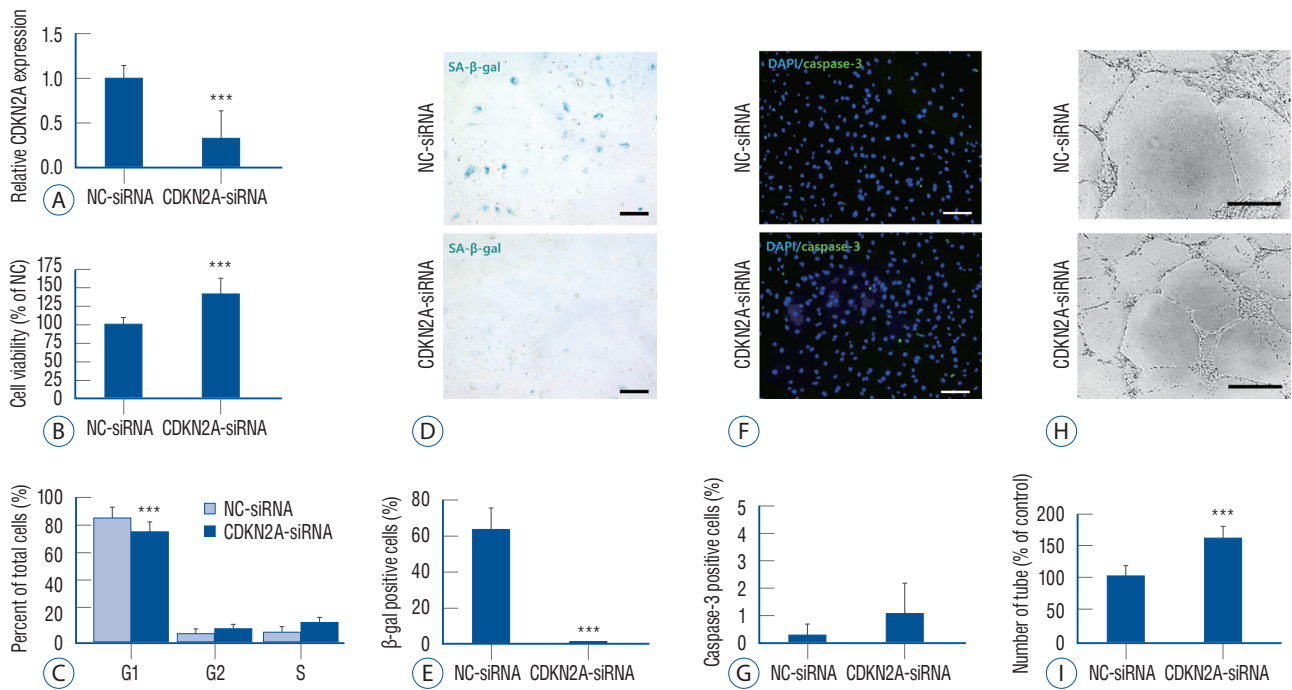


**Fig. 3.** Inhibition effect of CDKN2A in MMD ECFCs. A : CDKN2A-siRNA treatment effectively reduces CDKN2A mRNA expression by 70%. B : Cell viability analysis reveals increased cell growth of MMD ECFCs by knockdown of CDKN2A. C : Cell cycle analysis confirms inhibition of G1 arrest by knockdown of CDKN2A in MMD ECFCs. D and E : Senescence-associated β-galactosidase (SA-β-gal) assay (x100) shows a significantly decreased the cellular senescence of MMD ECFCs by knockdown of CDKN2A. F and G : Caspase-3 staining (x100) indicates that knockdown of CDKN2A does not affect apoptosis in MMD ECFCs. H and I : Tube formation analysis demonstrates that knockdown of CDKN2A significantly improves the tubule formation capability of MMD ECFCs (x100). Scale bars : 100 μm. \*\*\**p*<0.001. CDKN2A : cyclin-dependent kinase inhibitor 2A, NC: negative control, MMD : Moyamoya disease, ECFCs : endothelial colony-forming cells.

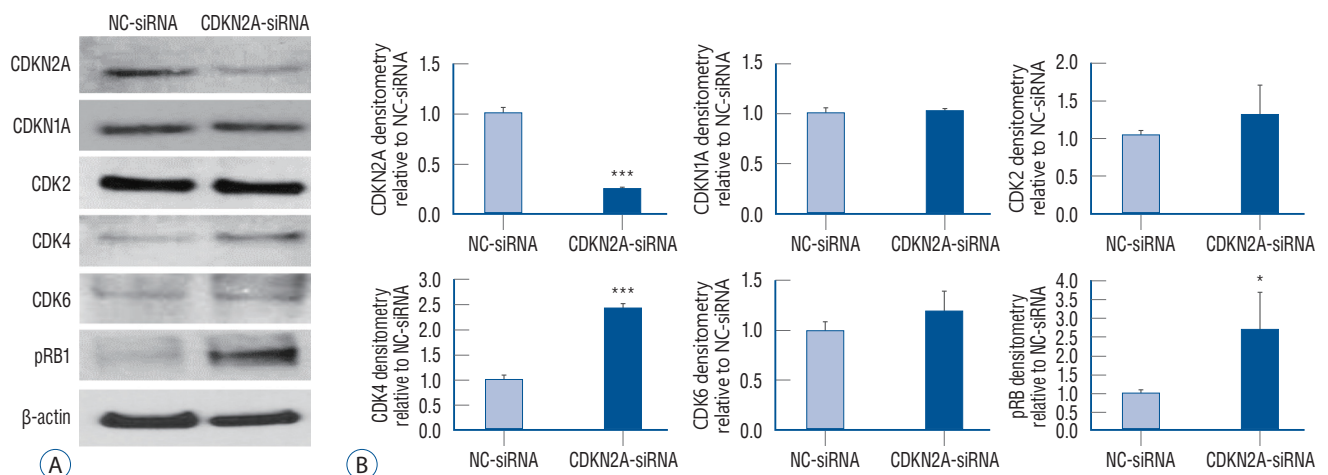


**Fig. 4.** Cellular senescence and cell cycle-related signaling pathways affected by inhibition of CDKN2A in MMD ECFCs. A : Representative western blot results indicate a significant increase in CDK4 and pRB by knockdown of CDKN2A in MMD ECFCs at 24 hours. On the other hand, CDKN1A, CDK2, and CDK6 are not affected by the knockdown of CDKN2A in MMD ECFCs. B : Densitometry graphs of the western blots are quantified, and the data are expressed as the mean±standard deviation. \**p*<0.05, \*\*\**p*<0.001. NC : negative control, CDKN2A : cyclin-dependent kinase inhibitor 2A, pRB1 : phospho retinoblastoma1, MMD : Moyamoya disease, ECFCs : endothelial colony-forming cells.

correlated with CDKs. The results showed that CDKN2A inhibition increased the protein expression of CDK4 and pRB by 2.4- and 2.7-fold, respectively (all  $p < 0.05$ , Fig. 4B). However, significant differences were not observed in the expression of CDKN1A, CDK2, and CDK6. Our data suggest that CDKN2A inhibition might regulate signaling pathways associated with cell cycle arrest and senescence by leading to upregulation of CDK4 and pRB.

## DISCUSSION

Our study suggested that CDKN2A, which is overexpressed in MMD ECFCs, regulates cell cycle arrest and senescence, thus leading to dysfunctions such as cell proliferation and tubule formation ability.

Basic research on MMD is challenging because of its rare incidence, low mortality rate, limited availability of surgical specimens from the affected internal carotid artery, and lack of animal models. Due to these limitations, peripheral blood from patients have been studied to investigate the pathogenesis of MMD. In particular, although ECFCs obtained from MMD PBMNCs have been studied for a long time, the levels of ECFCs in MMD remains controversial. A decreased numbers of ECFCs with defective functions have been observed in pediatric patients with MMD<sup>9</sup>), while increased levels of EPC in MMD have been reported<sup>19</sup>). Therefore, the number, quantity, and function of MMD ECFCs must be explicitly determined.

We isolated PBMNCs from pediatric MMD blood (2010–2020), cultured ECFCs and observed the following findings. No significant differences between MMD and normal was observed in the total number of PBMNCs. However, obtaining ECFCs by differentiating MMD PBMNCs and maintaining their characteristic's during culturing was difficult. Interestingly, once differentiated, the MMD ECFCs did not differ from normal ECFCs in ac-LDL uptake and surface marker expression. However, significant differences were observed in the functional aspects of normal ECFCs and MMD ECFCs. Compared to normal ECFCs, functional impairment of MMD ECFCs was observed. In particular, because of the reduced proliferation capacity of MMD ECFCs, cell subculturing was constrained, which increased the difficulty of obtaining sufficient amounts of cells for further experiments. Along

with the decreased cell proliferation, G1 cell cycle arrest, cellular senescence and decreased angiogenic capacity were also observed in MMD ECFCs compared to normal ECFCs. To elucidate the major factors regulating this aspect, we performed a biological pathway analysis and confirmed that the cell cycle was the most significant. Among the cell cycle genes, we found that CDKN2A was the most significantly overexpressed. One of the prominent features of cellular senescence is cell cycle arrest<sup>25</sup>), and CDKN2A upregulation is the main event in the ultimate phase of growth arrest in senescence<sup>20</sup>). CDK inhibitors, including CDKN2A and CDKN1A, are major cell cycle regulators, with CDKN2A acting at the G1 phase and blocking CDK activity<sup>23</sup>). We demonstrated whether the functional recovery of MMD ECFCs is possible through the regulation of CDKN2A. To elucidate the function of CDKN2A in MMD ECFCs, siRNA was used to inhibit CDKN2A. As expected, inhibition of CDKN2A improved the cell proliferation and tubule formation ability of MMD ECFCs while reducing cellular senescence and cell cycle arrest<sup>8</sup>). Additionally, we identified cell cycle-related signaling pathways by inhibition of CDKN2A, and the western blot results showed that CDK4 and pRB were increased while CDKN1A, CDK2 and CDK6 did not show significant effects.

The accumulation of senescent cells contributes to age-related disorders, neurodegenerative diseases, cardiovascular dysfunction, respiratory disease, cancers, and other chronic diseases. Senolytics, which selectively eliminate senescent cells, have been a potential therapeutic option for these various diseases. Cellular senescence is mediated at three points : 1) clearance of senescent cells, 2) inhibition of production of senescence-associated secretory phenotype factors<sup>26</sup>), and 3) targeting of senescent cell anti-apoptotic pathways<sup>11</sup>). The first human clinical trial of senolytics showed improvements of physical function in patients with idiopathic pulmonary fibrosis after treatment with dasatinib and quercetin<sup>7</sup>). Dasatinib and quercetin reduced senescent cell burden in adipose tissue in patients with diabetic kidney disease<sup>5</sup>). Clinical trials using novel flavonoid senolytics such as fisetin as well as dasatinib and quercetin are planned in Alzheimer's disease and COVID-19<sup>26</sup>).

We observed a decrease in angiogenic capacity and CDKN2A overexpression in MMD ECFCs, and confirmed that CDKN2A knockdown ameliorated the proliferative dysfunction of ECFCs. This suggest that the senescent state of ECFCs



is associated with the expression of the MMD phenotype. In MMD, the use of senolytics may be considered as adjunctive therapy after bypass surgery, which is currently the standard treatment. For clinical application, preclinical studies on efficacy and safety verification including off-target side effects should be preceded.

The limitations of our research include the lack of age matching when blood was obtained from normal and MMD patients (because obtaining blood from healthy children is ethically almost impossible) and the absence of an *in vivo* study. Moreover, since most of the MMD ECFCs for which sufficient cells were obtained for the experiment in this study were RNF213 GA, the relevance between the RNF213 variant and CDKN2A has unfortunately not been elucidated.

## CONCLUSION

Our results suggest that CDKN2A overexpression in MMD ECFCs induces cell cycle arrest and cellular senescence, resulting in decreased cell proliferation and angiogenesis capacity of MMD ECFCs. Therefore, modulation of CDKN2A may restore the function of MMD ECFCs.

## AUTHORS' DECLARATION

### Conflicts of interest

No potential conflict of interest relevant to this article was reported.

### Informed consent

Informed consent was obtained from all individual participants included in this study.

### Author contributions

Conceptualization : SAC, SKK; Data curation : SAC, YJM; Formal analysis : SAC, YJM, EJK; Funding acquisition : SKK; Methodology : SAC, YJM ; Project administration : SAC; Visualization : SAC, YJM; Writing - original draft : SAC, YJM, EJK; Writing - review & editing : SAC, YJM, JHP, JYL, KHK, SKK

## Data sharing

Data supporting the results of this study are provided at the request of the corresponding author. Data is not publicly available due to privacy or ethical restrictions.

## Preprint

None

## ORCID

Seung Ah Choi	<a href="https://orcid.org/0000-0003-4698-6445">https://orcid.org/0000-0003-4698-6445</a>
Youn Joo Moon	<a href="https://orcid.org/0000-0002-2965-4281">https://orcid.org/0000-0002-2965-4281</a>
Eun Jung Koh	<a href="https://orcid.org/0000-0002-4169-9546">https://orcid.org/0000-0002-4169-9546</a>
Ji Hoon Phi	<a href="https://orcid.org/0000-0002-9603-5843">https://orcid.org/0000-0002-9603-5843</a>
Ji Yeoun Lee	<a href="https://orcid.org/0000-0003-0464-7605">https://orcid.org/0000-0003-0464-7605</a>
Kyung Hyun Kim	<a href="https://orcid.org/0000-0002-8238-2043">https://orcid.org/0000-0002-8238-2043</a>
Seung-Ki Kim	<a href="https://orcid.org/0000-0002-0039-0083">https://orcid.org/0000-0002-0039-0083</a>

## • Acknowledgements

This work was supported by the National Research Foundation of Korea (NRF) grant funded by the Korea government (MSIT, 2019R1A2C209009911), and SNUH Kun-hee Lee Child Cancer & Rare Disease Project, Republic of Korea (grant number : 70-2023-3111).

## • Supplementary materials

The online-only data supplement is available with this article at <https://doi.org/10.3340/jkns.2023.0005>.

## References

1. Bang OY, Fujimura M, Kim SK : The pathophysiology of moyamoya disease: an update. **J Stroke** 18 : 12-20, 2016
2. Chang TY, Tsai WC, Huang TS, Su SH, Chang CY, Ma HY, et al. : Dysregulation of endothelial colony-forming cell function by a negative feedback loop of circulating miR-146a and -146b in cardiovascular disease patients. **PLoS One** 12 : e0181562, 2017
3. Choi SA, Chong S, Kwak PA, Moon YJ, Jangra A, Phi JH, et al. : Impaired functional recovery of endothelial colony-forming cells from moyamoya disease in a chronic cerebral hypoperfusion rat model. **J Neurosurg Pediatr** 23 : 204-213, 2018
4. Guey S, Tournier-Lasserre E, Hervé D, Kossorotoff M : Moyamoya dis-

- ease and syndromes: from genetics to clinical management. **Appl Clin Genet** **8** : 49-68, 2015
5. Hickson LJ, Langhi Prata LGP, Bobart SA, Evans TK, Giorgadze N, Hashmi SK, et al. : Senolytics decrease senescent cells in humans: preliminary report from a clinical trial of Dasatinib plus Quercetin in individuals with diabetic kidney disease. **EBioMedicine** **47** : 446-456, 2019
  6. Jangra A, Choi SA, Koh EJ, Moon YJ, Wang KC, Phi JH, et al. : Panobinostat, a histone deacetylase inhibitor, rescues the angiogenic potential of endothelial colony-forming cells in moyamoya disease. **Childs Nerv Syst** **35** : 823-831, 2019
  7. Justice JN, Nambiar AM, Tchkonja T, LeBrasseur NK, Pascual R, Hashmi SK, et al. : Senolytics in idiopathic pulmonary fibrosis: results from a first-in-human, open-label, pilot study. **EBioMedicine** **40** : 554-563, 2019
  8. Kang HS, Wang KC, Kim SK : Circulating vascular progenitor cells in moyamoya disease. **J Korean Neurosurg Soc** **57** : 428-431, 2015
  9. Kim JH, Jung JH, Phi JH, Kang HS, Kim JE, Chae JH, et al. : Decreased level and defective function of circulating endothelial progenitor cells in children with moyamoya disease. **J Neurosci Res** **88** : 510-518, 2010
  10. Kim SK, Cho BK, Phi JH, Lee JY, Chae JH, Kim KJ, et al. : Pediatric moyamoya disease: an analysis of 410 consecutive cases. **Ann Neurol** **68** : 92-101, 2010
  11. Kirkland JL, Tchkonja T : Cellular senescence: a translational perspective. **EBioMedicine** **21** : 21-28, 2017
  12. Lee JY, Moon YJ, Lee HO, Park AK, Choi SA, Wang KC, et al. : Deregulation of retinaldehyde dehydrogenase 2 leads to defective angiogenic function of endothelial colony-forming cells in pediatric moyamoya disease. **Arterioscler Thromb Vasc Biol** **35** : 1670-1677, 2015
  13. Liu W, Morito D, Takashima S, Mineharu Y, Kobayashi H, Hitomi T, et al. : Identification of RNF213 as a susceptibility gene for moyamoya disease and its possible role in vascular development. **PLoS One** **6** : e22542, 2011
  14. Ma Q, Xu Y, Liao H, Cai Y, Xu L, Xiao D, et al. : Identification and validation of key genes associated with non-small-cell lung cancer. **J Cell Physiol** **234** : 22742-22752, 2019
  15. Medina RJ, Barber CL, Sabatier F, Dignat-George F, Melero-Martin JM, Khosrotehrani K, et al. : Endothelial progenitors: a consensus statement on nomenclature. **Stem Cells Transl Med** **6** : 1316-1320, 2017
  16. Oh JW, Oh YJ, Han S, Her NG, Nam DH : High-content analysis-based sensitivity prediction and novel therapeutics screening for c-Met-addicted glioblastoma. **Cancers (Basel)** **13** : 372, 2021
  17. Phi JH, Choi SA, Lim SH, Lee J, Wang KC, Park SH, et al. : ID3 contributes to cerebrospinal fluid seeding and poor prognosis in medulloblastoma. **BMC Cancer** **13** : 291, 2013
  18. Phi JH, Suzuki N, Moon YJ, Park AK, Wang KC, Lee JY, et al. : Chemokine ligand 5 (CCL5) derived from endothelial colony-forming cells (ECFCs) mediates recruitment of smooth muscle progenitor cells (SPCs) toward critical vascular locations in moyamoya disease. **PLoS One** **12** : e0169714, 2017
  19. Rafat N, Beck GCh, Peña-Tapia PG, Schmiedek P, Vajkoczy P : Increased levels of circulating endothelial progenitor cells in patients with moyamoya disease. **Stroke** **40** : 432-438, 2009
  20. Regnault V, Challande P, Pinet F, Li Z, Lacolley P : Cell senescence: basic mechanisms and the need for computational networks in vascular ageing. **Cardiovasc Res** **117** : 1841-1858, 2021
  21. Roder C, Nayak NR, Khan N, Tagatiba M, Inoue I, Krschek B : Genetics of moyamoya disease. **J Hum Genet** **55** : 711-716, 2010
  22. Schira-Heinen J, Czapl A, Hendricks M, Kloetgen A, Wruck W, Adjaye J, et al. : Functional omics analyses reveal only minor effects of microRNAs on human somatic stem cell differentiation. **Sci Rep** **10** : 3284, 2020
  23. Sherr CJ, Roberts JM : CDK inhibitors: positive and negative regulators of G1-phase progression. **Genes Dev** **13** : 1501-1512, 1999
  24. Urbich C, Dimmeler S : Endothelial progenitor cells: characterization and role in vascular biology. **Circ Res** **95** : 343-353, 2004
  25. Wang HH, Lee YN, Su CH, Shu KT, Liu WT, Hsieh CL, et al. : S-phase kinase-associated protein-2 rejuvenates senescent endothelial progenitor cells and induces angiogenesis in vivo. **Sci Rep** **10** : 6646, 2020
  26. Wissler Gerdes EO, Misra A, Netto JME, Tchkonja T, Kirkland JL : Strategies for late phase preclinical and early clinical trials of senolytics. **Mech Ageing Dev** **200** : 111591, 2021
  27. Witt G, Keminer O, Leu J, Tandon R, Meiser I, Willing A, et al. : An automated and high-throughput-screening compatible pluripotent stem cell-based test platform for developmental and reproductive toxicity assessment of small molecule compounds. **Cell Biol Toxicol** **37** : 229-243, 2021
  28. Yu J, Du Q, Hu M, Zhang J, Chen J : Endothelial progenitor cells in moyamoya disease: current situation and controversial issues. **Cell Transplant** **29** : 963689720913259, 2020